Sensitivity Enhancement in 1D Heteronuclear NMR Spectroscopy via Single-Scan Inverse Experiments

Mor Mishkovsky and Lucio Frydman*[a]

Measuring the nuclear magnetic resonance spectra of low-γ heteronuclei such as ^{15}N constitutes an important analytical tool for the characterization of molecular structure and dynamics. The reduced resonance frequencies and magnetic moments of these heteronuclei, however, make the sensitivity of this kind of spectroscopy inherently lower than that of comparable ^{1}H NMR observations. A well-known solution to this sensitivity problem is indirect detection: a 2D NMR technique capable of enhancing the sensitivity of heteronuclear NMR by porting the actual data acquisition from the low-γ nucleus to neighboring protons. This has become the standard method of observation in biomolecular NMR, where the resolution introduced by 2D spectroscopy is always a sought-after commodity. Indirect detection, however, has not gained a wide appeal in organic chemistry or in in vivo investigations, where one-dimensional heteronuclear NMR information usually suffices. The present study explores the possibility of retaining certain advantages derived from indirect detection while not giving up on the simple one-dimensional nature of heteronuclear NMR, by relying on the spatial-encoding scheme we have recently demonstrated for implementing single-scan multidimensional NMR spectroscopy. Preliminary results based on a 1D modification of this experiment confirm theoretical calculations suggesting that the sensitivity of 1D ^{15}N NMR can be enhanced significantly in this manner; the relevance of this experiment given the advent of dedicated ^{1}H-observing cryogenic probeheads with very high sensitivities is briefly discussed.

Introduction

NMR spectroscopy serves as an important tool for studying the structure and dynamics of molecules.[1] One-dimensional (1D) NMR in particular underlies several key areas of contemporary analytical spectroscopy, which range in applications from organic and pharmaceutical chemistry to in vivo medical diagnosis. 1D NMR measures the resonance frequency of various nuclei in a molecule, providing the basic chemical shift and J-coupling information from which structural and dynamic information can become available. ^{15}N NMR in particular has been recognized as having great potential and plays important roles in both modern industry and academia.[2] One of the drawbacks of implementing experiments on this isotope, as well as on other nuclei I with small magnetogyric ratios γ_I, is the poorer signal-to-noise ratios (S/N) that characterize them in comparison to ^{1}H NMR. Still, the advent of Fourier transform NMR and of other forms of signal enhancement has made this kind of spectroscopy feasible and eventually routine.[2,3] Foremost among the signal enhancement techniques used in ^{15}N NMR is the INEPT pulse sequence, whereby all the heteronuclear polarization arises via a J-mediated transfer from the protons and thus an optimum enhancement factor γ_H/γ_I is obtained.[4] Even with the use of INEPT, however, the signal intensities measured in directly detected 1D heteronuclear NMR experiments remain smaller than their ^{1}H counterparts by approximately $(\gamma_H/\gamma_I)^2$: a factor γ_H/γ_I which reflects the smaller magnetic moments of the heteronuclei, and another γ_H/γ_I factor which is a consequence of the higher Larmor frequency in which, for a given external field strength, the ^{1}H NMR acquisition takes place.[5]

During the development of 2D NMR as a tool for biomolecular investigations, it was unambiguously demonstrated that the ensuing S/N penalty could be overcome if heteronuclear experiments were carried out in "inverse-detection" mode; that is, if the heteronuclear evolution were encoded along the indirect domain of a 2D experiment, and this information then passed over to a neighboring ^{1}H on which the actual measurement would take place.[6,7] Although indirect detection eventually became the standard approach to obtain ^{1}H/heteronuclear 2D correlations,[8] this mode of operation found limited application toward the acquisition of 1D NMR spectra. The reason for this probably lies in the fact that the organic/pharmaceutical chemist or the in vivo spectroscopist seeking ^{15}N/^{13}C information from synthetic or metabolic molecules is usually not interested in investing in the longer acquisition times that characterize 2D over 1D forms of spectroscopy, or in seeking the additional spectral resolution associated with spreading the resonances throughout a 2D rather than a 1D frequency space. Still, it is the purpose of the present article to discuss the possibility of retaining some of the indirect-detection sensitivity advantages while not forfeiting the single-scan or unidimensional nature of heteronuclear acquisitions; a potential made possible by the advent of spatially encoded acquisition methods capable of providing 2D NMR information within a single scan.[9,10]

[a] M. Mishkovsky, Prof. L. Frydman
Department of Chemical Physics, Weizmann Institute of Science
76100 Rehovot (Israel)
Fax: (+972) 8-9344123
E-mail: lucio.frydman@weizmann.ac.il

Principles of 1D Indirect Heteronuclear NMR Acquisitions

As has been discussed elsewhere in detail,[9] ultrafast 2D NMR enables the acquisition of 2D spectra within a single scan by replacing the usual t_1 time encoding with an analogous spatial encoding of the internal spin interactions. This can be achieved in a number of different ways,[10–12] the simplest of which involves the application of frequency selective pulses at variable offsets O_i while in the presence of a longitudinal excitation gradient G_e (Figure 1A). Indirect-domain frequencies Ω_1 become
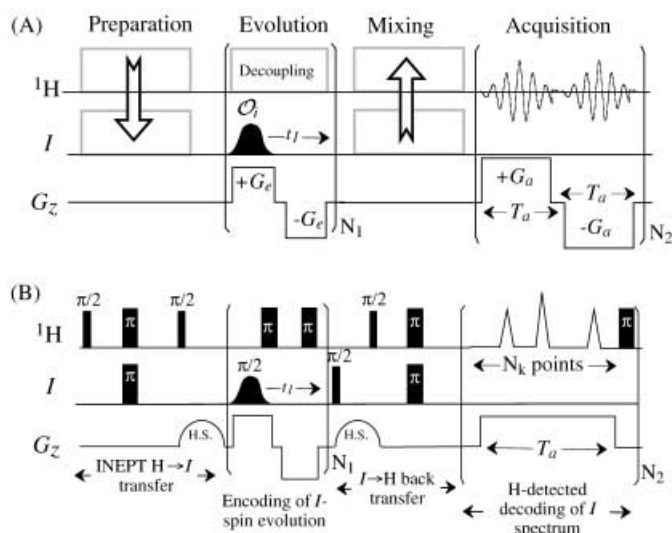

Figure 1. (A) Generic scheme of an indirectly detected ultrafast 2D NMR experiment. Following an initial polarization of the low-γ nucleus, a spatial encoding of the I-spin evolution is imposed by applying a train of N_1 frequency-shifted pulses with offsets $\{O_i\}_{1 \leq i \leq N_1}$. Such winding of the coherences is then transferred back to the sensitive ${}^1H$ nuclei where it becomes periodically decoded by an oscillating acquisition gradient G_a scanning the indirect-domain k/v_1 frequency axis, while the proton evolution becomes encoded as a function of t_2. (B) Adaptation of the spatially encoded scheme in (A) to the indirect acquisition of low-γ NMR spectra. For the sake of precision the actual pulse sequence used throughout this paper is illustrated; it is based on the spatially encoded single-scan 2D HSQC sequence described elsewhere,[10] with the acquisition modified by the addition of a spin-echo train and the use of monopolar G_a gradients.

thus encoded along a spatial domain according to discrete evolution phases $\{\phi_j = C\Omega_1(z_j - z_{N_1})\}_{j=0,N_1-1}$. The resulting winding of magnetizations can then be periodically decoded during the course of the acquisition time t_2 by applying an oscillating magnetic field gradient G_a, which imparts on the spins an additional phase factor $\phi(k) = kz = \left[\int_0^{t_2} G_a(t')dt'\right]z$. This additional phase factor translates the indirect-domain frequencies into echoes along the k domain, which appear at $k = -C\Omega_1$; when monitored as a function of the acquisition time t_2 and Fourier-transformed against this variable, such echoes yield the desired 2D correlation spectrum. As mentioned elsewhere, the resulting principles are general and can be used to record any nD NMR experiment within a single transient,[13] including indirectly detected heteronuclear I-${}^1H$ 2D NMR correlations where

echoes along the k domain reflect the I-spin chemical shift frequencies.[11]

For the purpose of this study we consider what would happen if the information being sought were not two-dimensional in nature but rather one-dimensional, and consisted of the 1D NMR spectrum of the insensitive I-spin nucleus. A potential new approach to retrieving this kind of 1D information could then rely on "suspending" the spin evolution of the detected protons along the direct domain of single-scan 2D heteronuclear NMR experiments, as would result for instance from the application of a train of refocusing π pulses removing the ${}^1H$ NMR evolution during t_2. When considered within the setting of a single-scan 2D HSQC experiment,[8] this collapsing of the information into a heteronuclear dimension could be carried out by the simple modification illustrated in Figure 1B. The resulting sequence is composed of an initial INEPT block, whereby ${}^1H$ z magnetization (H_z) is coherently transformed into two-spin $2H_zI_z$ spin order, a frequency-selective train of I pulses which, in combination with a bipolar field gradient, encodes the spin evolution of these spins along the sample's spatial orientation, a second INEPT-like period where this I-spin encoding is transferred back to protons via a two-spin order state, and a final acquisition period which combines a monopolar decoding gradient with a train of N_2 ${}^1H$ π pulses that effectively freezes both the ${}^1H$ chemical shift as well as the ${}^1H$-I spin coupling evolution.[1] The final train of refocusing pulses would then allow for the acquisition of a large number (N_2) of equivalent I-spin spectra within a single scan; all these spectra could then be co-added for the sake of improving the overall S/N. We explore next the potential sensitivity enhancement that the resulting single-scan 1D approach could achieve towards the acquisition of heteronuclear NMR spectra.

Signal-to-Noise Considerations: Indirect versus Direct 1D NMR Acquisitions

As explained elsewhere, ultrafast NMR pays a price for the sake of completing the multidimensional acquisition within a single scan, and that price consists of an increase in the noise that is observed in relation to a conventional 1D single-scan experiment.[9, 10] This derives from the need of this spatially encoded scheme to open up the spectrometer's filter bandwidth wide enough to allow for a fast simultaneous sampling of multiple dimensions. Thus, it is not evident that an indirect detection 1D experiment based on this kind of scheme will necessarily bring an enhanced sensitivity per unit time, and in fact we find that often it may not. Still, it can be shown that for sufficiently large (γ_H/γ_I) ratios, for instance those characterizing an ${}^{15}N$ NMR experiment, a sensitivity benefit can actually be derived from relying on a scheme like the one shown in Figure 1B. Showing this requires, in turn, a S/N comparison between direct and indirect acquisition modes, a comparison

---

[1] This strategy will still leave active modulations from homonuclear ${}^1H$–${}^1H$ couplings that might reflect in sensitivity losses. A variety of more complex refocusing strategies could then be used to take care of such couplings, yet for simplicity we neglect such issues in this study.

which is complicated by the fact that in a conventional experiment the acquisition will take place in the time-domain and at the *I*-spin Larmor frequency, whereas in the indirectly detected experiments spectra will arise directly in the frequency k/ν_1 domain and be detected at the ¹H Larmor frequency. Still, we attempt to derive in this section the approximate conditions under which such a 1D spatially encoded scheme might prove to be more sensitive than counterparts based on the direct detection of the *I*-spin time-domain signal.

To even out our S/N comparison we shall assume that both the directly and indirectly detected acquisition schemes share a number of commonalities: that they involve an equal number of spins, rely on similar pre-evolution enhancement schemes (usually an INEPT-type transfer), and that in both of them the *I* evolution occurs while in the presence of proton decoupling. We shall also make an electronics-related assumption, that is that for a given filter bandwidth (FB) of the NMR audio receiver the noise $N(t)$ picked up by the receiver coil will be given by Equation (1),[3]

$$N(t) = n(t)\sqrt{FB} = n(t)/\sqrt{\Delta t} \tag{1}$$

where Δt is the physical dwell time, and $n(t)$ is a statistically random noise function characterized by a root-mean-square (r.m.s.) amplitude σ_N, which incorporates parameters such as the coil's resistance, Q value, etc. We proceed then with an analysis of the S/N expected for the new indirectly detected acquisition scheme hereby proposed. The signal in this case will be given by the sum of N_2 indirectly detected data sets $[s_{id}(k)]_j$, identical in principle to one another except for the effects of a T_2^H relaxation decay that affects the ¹H signal over the course of the acquisition.[2] The overall indirectly detected *I*-spin signal arising from this sum can therefore be expressed by Equation (2)

$$\begin{aligned} S_{id}(k) &= \sum_{j=1}^{N_2} [s_{id}(k)]_j \approx s_{id}(k) \sum_{j=1}^{N_2} \exp[-t_j/T_2^H] \\ &= N_2 s_{id}(k)\langle E(T_2^H)\rangle \end{aligned} \tag{2}$$

where t_j indicates the time elapsed between the beginning of the acquisition and the approximate instant when the *j*-th spectrum $(1 \leq j \leq N_2)$ was acquired, and the final bracketed term $\langle E(T_2^H)\rangle$ summarizes a relaxation-derived attenuation factor depending on T_2^H and on the overall indirect-detecttion data acquisition time AT_{id}. This $S_{id}(k)$ spectrum will adopt different values depending on the k/ν_1 frequency considered; its maximum will be achieved at the position $k=|C\Omega_I|$, where Ω_I is the *I*-spin chemical shift value. As explained elsewhere, this signal will encompass the coherent superposition of magnetizations from all spins that reside in the sample;[10] we define the time-domain signal intensity at this condition as s_{id}^0. As for the noise N_{id} that will characterize these indirectly detected data, it will

be given simply by the addition of the statistically independent N_2 noise contributions being summed for each k value. Following Equation (1) this results in Equation (3).

$$N_{id}(k) = \sum_{j=1}^{N_2} [N(k+jT_a)] = \frac{1}{\sqrt{\Delta t}} \sum_{j=1}^{N_2} n(t_j) = \sqrt{\frac{N_2}{\Delta t}}\sigma_n \tag{3}$$

Considering now that the overall data acquisition time for the indirectly detected experiments is $AT_{id}=N_2 N_k \Delta t$, with N_k being the number of points digitized per echo period T_a, it follows that the overall S/N (defined as the ratio between the maximum peak intensity over the noise's variance) will be given by Equation (4).

$$(S/N)_{id} = \frac{s_{id}^0}{\sigma_n}\langle E(T_2^H)\rangle \sqrt{\frac{AT_{id}}{N_k}} \tag{4}$$

As for a comparable S/N calculation for a conventional directly detected acquisition experiment, we shall assume as above that the time-domain *I*-spin signal is defined by an overall intensity s_{dd}^0, a frequency Ω_I, and an exponential decay time T_2^I [Equation (5)].

$$s_{dd}(t) = s_{dd}^0 \exp(i\Omega_I t)\exp(-t/T_2^I) \tag{5}$$

The discrete Fourier transformation of *NP* signal points sampled over an acquisition time AT_{id} then yields a maximum at a frequency $\nu=\Omega_I$, with a peak intensity [Equation (6)],

$$S_{dd} = \sum_{j=1}^{NP} |s_{dd}(t_j)| = s_{dd}^0 \sum_{j=1}^{NP} \exp\left[-t_j/T_2^I\right] = NP s_{dd}^0 \langle E(T_2^I)\rangle \tag{6}$$

where $t_j=\frac{j}{NP}AT_{dd}$ represents the instant of signal digitization, and the factor $\langle E(T_2^I)\rangle$ is akin to the one described earlier in the context of the ¹H-detected acquisition but involving the *I* spin. Concerning the noise N_{dd} in the neighborhood of this peak, we shall once again consider it to be derived from a random time-domain function whose amplitude is filter-bandwidth dependent. This leads to a direct analog of Equation (3) [Equation (7)].

$$N_{dd} = \frac{1}{\sqrt{\Delta t}} \sum_{j=1}^{NP} n(t_j) = \sqrt{\frac{NP}{\Delta t}}\sigma_n \tag{7}$$

Taking then the ratio between Equations (6) and (7) and using the fact that the data acquisition time in this kind of experiment will be given by $AT_{dd}=NP\cdot\Delta t$ results in the overall sensitivity expression [Equation (8)].

$$(S/N)_{dd} = \frac{s_{dd}^0}{\sigma_n}\langle E(T_2^I)\rangle \sqrt{AT_{dd}} \tag{8}$$

The sensitivities summarized by Equations (4) and (8) present a number of common features: they are independent of the actual dwell times, increase as the square root of the data acquisition time, and for a given acquisition time they are both affected by a rate of transverse relaxation, T_2. In principle one would assume that these last two parameters are considerably

---

[2] In fact, spectral data sets collected for even and odd *j* values $(1 \leq j \leq N_2)$ using the scheme in Figure 1B appear mirror-imaged and out-of-phase with each other, but these differences can be trivially corrected prior to summing up all N_2 data sets.

different for the ^{1}H- and the I-detected experiments, and play an important role in the sensitivity comparison. Indeed proton magnetizations are usually affected more severely than low-γ nuclei by instrumental inhomogeneities, and their signals decay faster than those of the latter. In the present context, however, we find that the reliance of the indirectly detected scheme in Figure 1B on a spin-echo train over the course of the acquisition largely erases these differences: the rates of transverse decay of the refocused ^{1}H and of the decoupled I transverse coherences are fairly similar, thereby similar acquisition times can be used in both types of experiments. The $\langle E(T_2)\rangle\sqrt{AT_{dd}}$ terms appearing in Equations (4) and (8) can thereby be factored out on making a comparison between (S/N)$_{id}$ and (S/N)$_{dd}$. Two main parameters then end up controlling the relative sensitivities of directly and indirectly detected schemes. One is the $\sqrt{N_k}$ term that scales down the sensitivity of the latter experiments; the other the s^0_{id}/s^0_{dd} ratio that defines the relative strengths of the time-domain signals elicited by the sample in indirectly and directly detected acquisition modes. It is from the competition between these two sizable factors that the new indirect-detection mode may or may not present advantages in relation to the usual way of collecting 1D NMR spectra from the I nuclei.

The $\sqrt{N_k}$ term is akin to the one affecting S/N in ultrafast 2D NMR experiments and for usual conditions it will lead to a considerable loss in terms of sensitivity. The s^0_{id}/s^0_{dd} ratio on the other hand contains the $(\gamma_H/\gamma_I)^2$ factor, which has made indirect-detection the favored mode of collecting 2D heteronuclear correlation data. The s^0_{id}/s^0_{dd} ratio is further affected by the relaxation decay that might have affected the anti-phase I coherence during the course of its free t_1 evolution, by a factor of the order of unity depending on the I-group multiplicity and on other details of the $I\rightarrow{}^1$H transfer, and by an instrumental factor f that describes how closely the receiving pick-up coils in the directly and indirectly detected acquisitions couple to the changing magnetic flux created by the precessing ^{1}H or I spins. This instrumental f factor is once again in the order of unity when considering indirectly and directly detected experiments carried out on probeheads optimized for ^{1}H or I-spin detection, respectively, but can be heavily biased towards proton sensitivity when considering specialized instrumentation such as cryogenically cooled or surface "inverse"-coil setups.

It turns out therefore that the potential sensitivity gain arising from the implementation of the indirectly detected 1D scheme will depend on the ratio between two relatively large quantities. For usual experimental conditions the $\sqrt{N_k}$ term will attenuate this detection mode by a factor of approximately 10–15.[3] This factor is comparable to the maximum benefit expected from the $(\gamma_H/\gamma_I)^2$ factor when attempting the detec-

tion of a ^{13}C NMR experiment, and the advantages in this case are consequently not immediately apparent. On the other hand the $(\gamma_H/\gamma_I)^2$ factor reaches 100 for ^{15}N NMR experiments; it was this kind of measurements that we consequently assayed.

Results and Discussion

To verify the potential of the alternative presented above for the collection of 1D heteronuclear NMR spectra, the pulse sequence sketched in Figure 1 coupled to the sum-over-FIDs (FIDs = free induction decays) processing protocol described in the previous section, was applied to $I={}^{15}$N nuclei using a [D$_6$]DMSO solution of ^{15}N-labeled urea. The left-hand panels in Figure 2 compare two single-scan time-domain data sets acquired on such solution using an initial INEPT enhancement of the ^{15}N: the top one involves an indirect ^{15}N detection via coupled protons as suggested in Figure 1B; the lower one is a conventional proton-decoupled direct detection of the ^{15}N signals. Both measurements were carried out on a Bruker DMX800 NMR spectrometer using identical dwell times and therefore the same effective filter bandwidths, using the only probehead available on the instrument: a QXI quadruple-resonance/triple-axis system. The sensitivity difference between the signal intensities in these two data sets is immediately evident upon inspecting the time-domain data on the left-hand panels, and its origin resides in the $s^0_{id}/s^0_{dd}\gg 1$ ratio characterizing this experiment and this observation probehead. Such impressive sensitivity gain displayed by the proton-detected time-domain data is tempered when calculating the corresponding NMR spectra due to the $\sqrt{N_k}$ sensitivity loss affecting the sum-of-spectra approach over the conventional direct-domain Fourier transform. Still, a clear sensitivity advantage in favor of the indirectly detected spectrum is visible when comparing the two sets (Figure 2, right-hand panels). Also worth noting is the much lower resolution affecting the indirectly over the directly detected spectral line shape, a consequence of the relatively weak field gradients available in the system and of the restricted number of individual ^{15}N elements that could therefore be excited. Optimizing these excitation details to narrow the k-space interferogram should sharpen up the resonances and thereby lead to an improvement in the spectral resolution. Yet by contrast to what happens when peaks are narrowed in conventional time-domain experiments, this resolution enhancement is not expected to bring about an increase in the overall peak intensity of the indirectly detected trace.[10] In fact a drop in the experiment's overall sensitivity could arise from the relaxation losses that might affect the evolving coherences during the longer evolution times to be involved. Still for most practical instances of interest $t_1 \ll T^H_1, T^N_2$; such losses can therefore be expected to be fairly minor, and thus we consider the degree of spectral resolution of secondary importance within the framework of the present sensitivity discussion.

To distinguish whether the large sensitivity enhancement evidenced on going from the top to the bottom traces of Figure 2 arises from the sizable $(\gamma_H/\gamma_N)^2$ factor associated with

---

[3] This in turn implies that 100–200 N_k points will characterize spectra along the k/ν_1 axis. This is more than sufficient under current experimental conditions where spectral resolution is dictated by the relatively small number of spatial elements which can be excited at the low-γ frequency, and is expected to suffice even when dealing with stronger gradients or more efficient excitation modes if coupled to zero-filling of the data in the conjugate (z) domain.
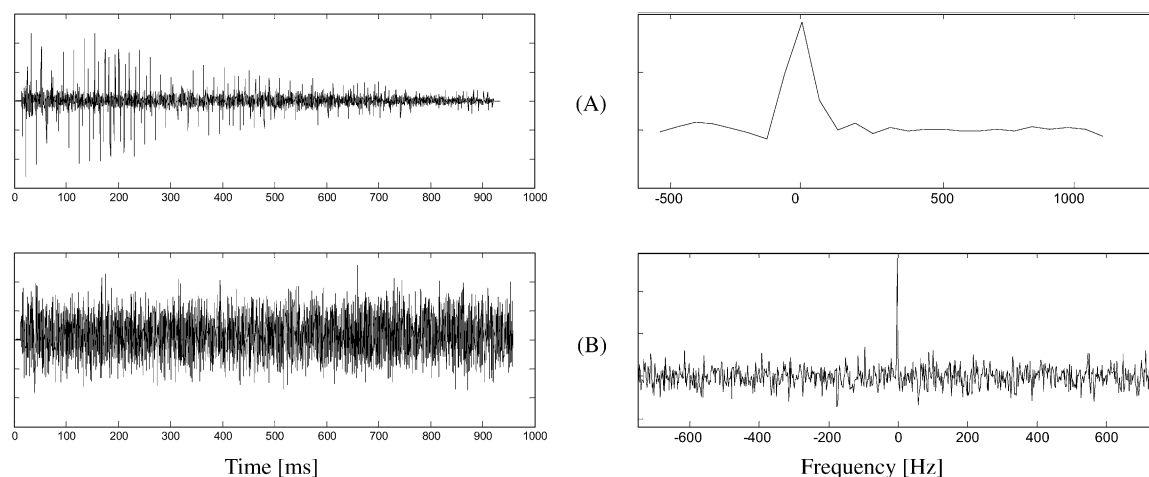
(A)

(B)

Time [ms]

Frequency [Hz]

Figure 2. *Comparison between optimized indirectly detected (A) and directly detected (B) ^{15}N NMR data sets obtained on a test 20 mM urea sample. Shown on the left-hand side panels are the time-domain sets as collected on an 800 MHz Bruker NMR spectrometer; right-hand side panels show spectra arising after suitable processing of the time-domain data. As described in the text, this processing involves separating the interleaved k-domain sets and adding them in a correct fashion for (A), a procedure including a time-reversal of the even-numbered spectra and proper phasing of even and odd sets. A conventional weighting with a decaying exponential ($T_2 = 1.5$ sec), zero-filling and Fourier transformation of the signal was involved in (B). Both time-domain sets were collected in a single transient using an initial INEPT enhancement of the ^{15}N magnetization, a 192 μs physical dwell time and approximately 4800 complex points. Other acquisition details for the indirect-detection include $N_1 = 16$, $N_k = 50$, $N_2 = 96$, $\Delta O = 2.6$ kHz, $G_e = 50$ G cm^{-1}, $G_a = 0.5$ G cm^{-1}, and a 0, 120, 0° phase cycling of the π-pulses involved in the spin-echo train.[14]*

the indirect detection mode or from a large instrumental f factor biasing sensitivity in favor of proton detection, a quantum mechanical simulation of the signals expected from both indirectly and directly detected experiments was carried out. These simulations took into account the time-propagation of a three-spin density-matrix system comprised of urea's nitrogen spin and its two bonded protons, manipulated under the exact same conditions as those employed in the indirectly and directly detected experiments. For simulating these experiments the calculation also partitioned the sample into a large number of Δz slices, to account for the potential spatial dependence of the various interactions involved. A match was then attempted between the data afforded by these simulations and the actual experimental signals observed, using as fitting variables the effective relaxation times T_2^H, T_2^N which affect the transverse decay of coherences during the acquisition of these two data sets, a random noise level whose amplitude solely depended on the dwell times that were used and, the instrumental factor f reflecting the potential bias of the NMR probehead towards indirect or direct detection. Results stemming from these simulations are summarized in Figure 3. Shown once again in Figure 3A is the experimental data set obtained in the proton-detection experiment prior to the summing up of the N_2 spectra (this time shown in absolute mode to convey a better idea of the signal's overall decay rate). Fitting of these data (Figure 3B) yields an effective T_2^H relaxation time of 490 ms and an arbitrary level of noise. Since the same dwell time was also used in the directly detected experiment, a similar noise level can be presumed for the conventional ^{15}N acquisition. However, superimposing such noise level onto an INEPT-enhanced ^{15}N FID arising from a quantum-mechanical simulation where the signal is already $(\gamma_H/\gamma_N)^2$ times lower due to the factors mentioned earlier (Figure 3C), will still yield an

S/N that is considerably higher than that which is experimentally observed (Figure 3E). This difference between expectation and experiment can be ascribed to the instrumental f factor biasing sensitivity in favor of the proton detection; the simulation requires attenuating the (S/N)$_{dd}$ by a factor $f \approx 2.9$ in order to match the quantum-mechanical expectation to the experiment (Figures 3D and 3E). This is a reasonable value considering that similar factors lengthen the duration of a given low-γ RF pulse width—for instance, $\pi/2$ pulse lengths applied on similarly tuned systems at comparable RF power levels- when going from a direct-detection to an indirect-detection probehead. Also worth remarking on is the fact that for small molecules such as the one under consideration the use of a spin-echo sequence indeed ends up lengthening the transverse proton relaxation times over those of the heteronucleus, which according to the simulations were 490 ms for the former and 200 ms for the latter.

Figure 4 displays an additional test on the potential sensitivity enhancement of indirect-detection experiments, once again monitoring an ^{15}N-enriched urea solution (20 mM in [D$_6$]DMSO) but this time on a different platform: a Varian iNova500 system incorporating a triple-axis/triple-resonance probehead. The fact that a different platform was used implies that slightly different spectral resolution, f-factors and acquisition times characterized the optimized indirectly and directly detected experiments. Such considerations notwithstanding, the indirect-domain spectra still evidenced an attractive enhancement in sensitivity, with the final spectrum showing a per-scan improvement factor approximately nine times higher than its directly detected counterpart. As a last example on the potential of this technique we illustrate in Figure 5 another application recorded on this spectrometer, this time involving two ^{15}N resonances arising from a solution of isotopically labeled Fmoc-
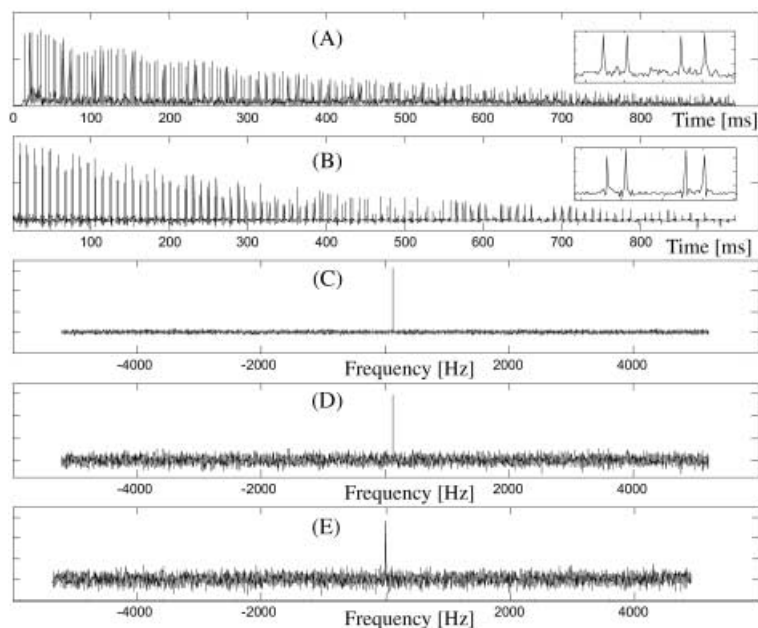
Figure 3. *Estimation of the sensitivity enhancement gain in indirectly versus directly detected ^{15}N NMR experiments by means of spin simulations. (A) Experimental directly detected INEPT-enhanced ^{15}N NMR data set (magnitude) used as initial S/N benchmark. (B) Best fit of the experimental data set, arising from a quantum-mechanical propagation of spins throughout the same experimental conditions as in (A), followed by multiplication of the final data set with an exponential decaying function to account for T_2 and by the addition of a suitable noise level. The slight differences noticeable between the baselines of traces (A) and (B) are artifacts arising from the magnitude display mode; the similar S/N that actually characterizes these two sets can be better appreciated from the zoomed insets, shown to the right of each trace, taken from the first two gradient echoes of each plot. Also, the slow modulation observed in the spin-echo train can be traced to the finite nature of the involved π pulses. (C) Directly detected ^{15}N NMR spectrum predicted from density matrix calculations including the preacquisition INEPT enhancement, should the same noise level as that used for trace (B) characterize such acquisition. (D) As in (C) but considering a noise level that is 2.9 times bigger. (E) Experimental ^{15}N NMR spectrum actually collected using direct detection, displaying a similar S/N as the one shown in panel (D).*

alanine and Fmoc-valine (Fmoc = 9-fluorenylmethoxy-carbonyl) in CDCl$_3$. Two peaks approximately 400 Hz apart originate from this solution on our 11.7 T system, with a signal-to-noise that is not sufficiently high enough to allow an optimized interactive tuning of the indirectly detected experiments (particularly of the all-important spin-echo train). Still, even under these less-than-ideal conditions, the application of indirect-detection yields a per scan sensitivity enhancement factor of approximately 20 over its directly detected counterpart.

Conclusions

The present study sought to explore the potential gains that newly developed ultrafast NMR protocols could bring to enhancing the sensitivity of heteronuclear NMR experiments. That sensitivity gains could result from this approach is not from the outset altogether clear, as ultrafast methodologies in their current implementation are known to suffer from a sizable $\sqrt{N_k}$ sensitivity attenuation. Still a number of factors can combine to overcome this attenuation, most important among them the $(\gamma_H/\gamma_I)^2$ enhancement characterizing the indirect detection. In the case of nuclei with low-enough γ ratios such as ^{15}N this is sufficient to compensate for the $\sqrt{N_k}$ sensitivity loss, which makes indirect detection a convenient approach to acquire 1D heteronuclear NMR spectra. From a practical standpoint two additional factors arise that can also favor the indirect detection mode. One is the instrumental factor f that biases the sensitivity of the detection towards proton experiments. Although this factor is entirely artificial its importance
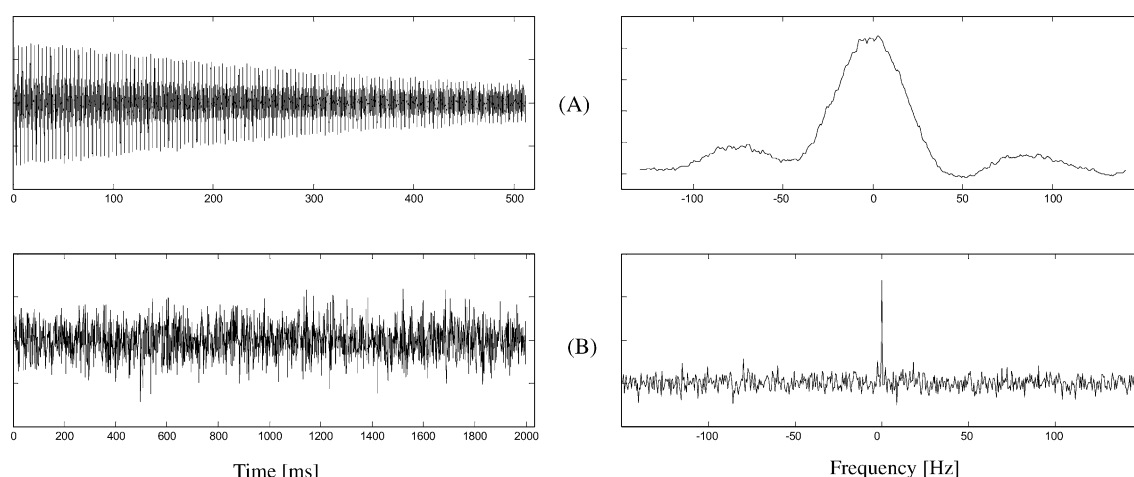

Figure 4. *As in Figure 2, but this time with the experiments recorded using a 500 MHz Varian NMR spectrometer on a 20 mm ^{15}N-enriched urea solution. Two scans with a {0, 180°} phase cycling of the 500-μs-long ^{15}N excitation pulses and of the receiver phase were collected in the indirectly detected experiment (A), whereas 8 phase cycled scans were collected in the INEPT-enhanced directly detected experiment (B). Other relevant details for the indirect-detection include $N_1 = 17$, $N_2 = 256$, $\Delta O = 2$ kHz, $G_e = 45$ G cm^{-1}, $G_a = 1$ G cm^{-1}, and an x–y phase cycling of the π-pulses involved in the spin-echo train[15] that in this case provided nearly ideal refocusing throughout the acquisition.*
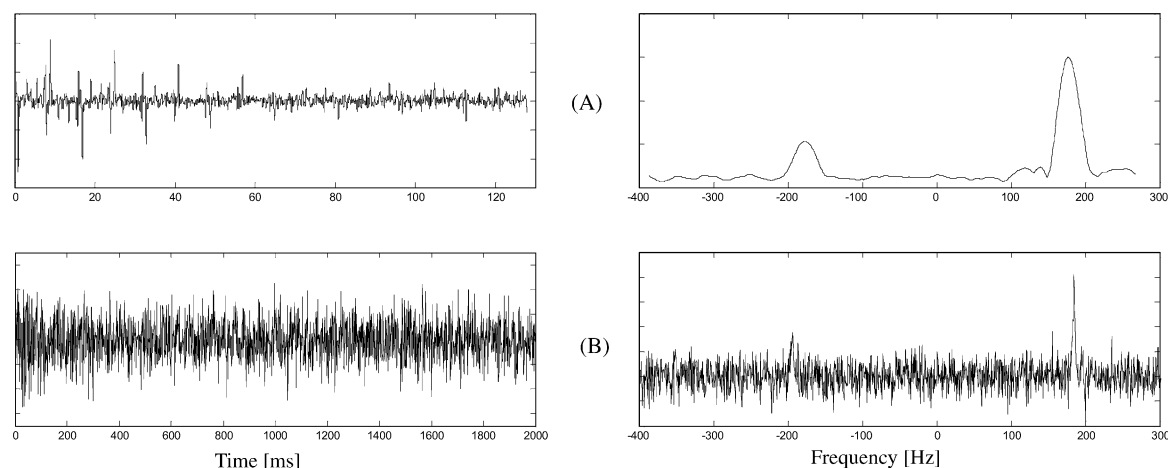
Figure 5. *As Figure 4 but on a 20 mM solution of ^{15}N-enriched alanine-Fmoc and valine-Fmoc. Four scans were collected in the indirectly detected experiment (A), while 32 scans were used in the directly detected set (B). Other relevant details for the indirect-detection experiment included $N_1 = 26$ excitation pulses 700-μs long each, $N_2 = 16$, $\Delta O = 1.8$ kHz, $G_e = 50$ G cm^{-1} and $G_a = 1.2$ G cm^{-1}.*

should not be underestimated, given the fact that both the high-field NMR as well as the MRI spectroscopy communities are increasingly relying on proton-oriented detection coils. This fact turns out to be of particular relevance ever since the advent of cryogenically cooled probes, expensive and high-maintenance instruments, which have left the traditional chemist interested in recording simple 1D heteronuclear NMR spectra searching for an answer with practical sensitivity. The indirect-detection mode here described might furnish one such alternative. In fact the advent of cryogenically cooled systems might tilt the sensitivity balance of 1D acquisitions toward indirect-detection modes even for higher-γ spins such as ^{13}C, as the signal enhancement in such systems could offset the higher S/N otherwise characterizing directly detected 1D spectra on conventional room-temperature probeheads.[4] A second factor worth mentioning upon examining the potential of indirect-mode detection is the reliance of the scheme in Figure 1B upon a spin-echo time-suspension of the ^{1}H evolution. On the basis of Fourier arguments such a procedure would seem unnecessary, as the peak intensities resulting from it should in principle be identical to those originating from a conventional ultrafast 2D HSQC acquisition. Yet by prolonging the effective lifetimes of ^{1}H transverse magnetizations and making them comparable to those of a natural heteronuclear decay, the spin-echo procedure contributes significantly to the overall competitiveness of the indirect-detection procedure. More sophisticated spin-echo procedures than the ones here employed, relying on more extensive supercycles, composite pulses, or refocusing strategies incorporating homonuclear *J*-decoupling, might provide additional gains in the final S/N that is observed. Another variant worth considering involves the use of long range *J*-mediated transfers, capable of bringing

into the realm of indirectly detected experiments heteronuclei that are not directly bound to protons.

The sensitivity enhancements illustrated in Figures 2–5 do not imply that 1D indirect-detection experiments have reached a stage mature enough to serve as the standard approach to record NMR spectra from ^{15}N or other low-γ nuclei in an organic or pharmaceutical chemistry setting. Indeed as spectra in these plots also reveal, our indirect-detection spectroscopic hardware is still unable to furnish the spatially encoded experiments with the kind of Hertz peak resolution and Kilohertz-wide spectral widths that the typical chemist looks for. As explained elsewhere in more detail, however, improvements in the gradient hardware might improve these characteristics.[10, 11] Gains could also result from using alternative modes of imparting on the spins their initial spatial encoding. In either case, improvements in the spectral resolution and range should result, without significantly affecting the gains achieved in terms of sensitivity. Research along these two parallel avenues is currently in progress.

Acknowledgments

Keywords: inverse detection · NMR spectroscopy · pulse sequences · relaxation · ultrafast 2D NMR

---

4 Of course a better alternative might be to collect ^{13}C NMR spectra on an optimized cryoprobe system, but so far these are available only in very specialized laboratories.

[1] *Encyclopedia of NMR* (Eds.: D. M. Grant, R. K. Harris), John Wiley & Sons, Chichester, **1996**.

[2] G. C. Levy, R. L. Lichter, *Nitrogen-15 Nuclear Magnetic Resonance Spectroscopy,* John Wiley & Sons, New York, **1979**.

[3] R. R. Ernst, G. Bodenhausen, A. Wokaun, *Principles of Nuclear Magnetic Resonance in One and Two Dimensions*, Clarendon, Oxford, **1987**.

[4] G. A. Morris, R. Freeman, *J. Am. Chem. Soc.* **1979**, *101*, 760–762.

[5] D. I. Hoult, *Progr. Nucl. Magn. Reson. Spectrosc.* **1978**, *12*, 41–77.

[6] L. Müller, *J. Am. Chem. Soc.* **1979**, *101*, 4481–4484.

[7] G. Bodenhausen, D. J. Ruben, *Chem. Phys. Lett.* **1980**, *69*, 185–189.

[8] J. Cavanagh, W. J. Fairbrother, A. G. Palmer III, N. J. Skelton, *Protein NMR Spectroscopy: Principles and Practice*, Academic Press, San Diego, **1996**.

[9] L. Frydman, T. Scherf, A. Lupulescu, *Proc. Natl. Acad. Sci. USA* **2002**, *99*, 15858–15862.

[10] L. Frydman, A. Lupulescu, T. Scherf, *J. Am. Chem. Soc.* **2003**, *125*, 9204–9217.

[11] B. Shapira, A. Lupulescu, Y. Shrot, L. Frydman, *J. Magn. Reson.* **2004**, *166*, 152–163.

[12] P. Pelupessy, *J. Am. Chem. Soc.* **2003**, *125*, 12345–12350.

[13] Y. Shrot, L. Frydman, *J. Am. Chem. Soc.* **2003**, *125*, 11385–11396.

[14] R. Tycko, H. M. Cho, E. Schneider, A. Pines, *J. Magn. Reson.* **1985**, *61*, 90–101.

[15] T. Gullion, D. B. Baker, M. Conradi, *J. Magn. Reson.* **1990**, *89*, 479–484.